Mon. Not. R. Astron. Soc. **000**, 1–?? (2014) Printed 5 September 2014 (MN LATEX style file v2.2)

The quiescent state of the accreting X-ray pulsar SAX J2103.5+4545

P. Reig[1,2⋆], V. Doroshenko[3] and A. Zezas[2,1]
[1]*IESL, Foundation for Research and Technology, 71110 Heraklion, Crete, Greece*
[2]*University of Crete, Physics Department, PO Box 2208, 710 03 Heraklion, Crete, Greece*
[3]*Institut für Astronomie und Astrophysik, Sand 1, 72076 Tübingen, Germany*

arXiv:1409.1398v1 [astro-ph.SR] 4 Sep 2014

Accepted ??. Received ??; in original form ??

ABSTRACT

We present an X-ray timing and spectral analysis of the Be/X-ray binary SAX J2103.5+4545 at a time when the Be star's circumstellar disk had disappeared and thus the main reservoir of material available for accretion had extinguished. In this very low optical state, pulsed X-ray emission was detected at a level of $L_X \sim 10^{33}$ erg s^{-1}. This is the lowest luminosity at which pulsations have ever been detected in an accreting pulsar. The derived spin period is 351.13 s, consistent with previous observations. The source continues its overall long-term spin-up, which reduced the spin period by 7.5 s since its discovery in 1997. The X-ray emission is consistent with a purely thermal spectrum, represented by a blackbody with $kT = 1$ keV. We discuss possible scenarios to explain the observed quiescent luminosity and conclude that the most likely mechanism is direct emission resulting from the cooling of the polar caps, heated either during the most recent outburst or via intermittent accretion in quiescence.

Key words: X-rays: binaries – stars: neutron – stars: binaries close –stars: emission line, Be

1 INTRODUCTION

SAX J2103.5+4545 belongs to the sub-class of high-mass X-ray binaries known as Be/X-ray binaries (BeXB). In these systems, a neutron star orbits around an OBe companion (Reig 2011). In a BeXB, the main source of matter available for accretion is the gaseous geometrically thin equatorial disk around the Be star. The disk is fed from the material lifted from the star's photosphere by a still uncertain mechanism. In classical (isolated) Be stars, there is growing evidence that the disk is Keplerian and supported by viscosity (Rivinius, Carciofi & Martayan 2013).

Most BeXBs are transient X-ray sources that exhibit outbursts when a compact object passes close or through the Be disk. Correlated optical/IR/X-ray variability is often observed on time scales of months or years and generally attributed to the extension of the circumstellar disk (Negueruela et al. 1998; Reig et al. 2007, 2010). The outburst activity is commonly divided in two types: type I outbursts are modulated by the orbital period of the system and occur when the neutron star passes close to the disk and accretes from its outer regions. The type II, or giant outbursts, exhibit higher X-ray luminosity close to the Eddington value $L_X \sim 10^{38}$ erg s^{-1}, and are usually associated with the accretion of a substantial part of the Be disk (Reig et al. 2007).

Several systems have also been observed in quiescence at X-ray luminosities in the range of $L_X \sim 10^{32} - 10^{34}$ erg s^{-1} (Schulz, Kahabka & Zinnecker 1995; Campana et al. 2002; Tomsick et al. 2011). However, pulsations were detected only in the brighter sources with longer spin periods, which are likely powered by accretion in quiescence (Mereghetti et al. 1987; Negueruela et al. 2000; Rutledge et al. 2007).

The compact object in SAX J2103.5+4545 is clearly a neutron star as the observed X-ray emission is pulsed. At the time of its discovery by *BeppoSAX* in February 1997, the pulse period was $P_{\rm spin} = 358.61 \pm 0.03$ s (Hulleman, in 't Zand & Heise 1998). Since then, the neutron star exhibits a general spin-up trend, although the rate of the period change has not remained constant. Occasionally, the long-term spin-up trend is interrupted by spin-down intervals (Ducci et al. 2008). The optical companion is a moderately reddened ($A_V = 4.2$ mag) V=14.2 B0Ve star (Reig et al. 2004).

The distance estimated from optical data is ∼6.5 kpc (Reig et al. 2004, 2010), while X-ray observations suggest a lower value of ∼4.5 kpc (Baykal et al. 2007). SAX J2103.5+4545 has a moderately eccentric orbit with $e = 0.4$ and an orbital period of 12.7 days (Baykal et al. 2007; Camero Arranz et al. 2007). Its relatively long spin period and relatively short orbital period locates SAX J2103.5+4545 in the wind-fed supergiant region of the $P_{\rm orb} - P_{\rm spin}$ diagram (Corbet 1986).

SAX J2103.5+4545 shows extended bright and faint X-ray states that last for several months (Reig et al. 2010). During the faint state, the X-ray intensity does not change significantly with orbital phase (Baykal, Stark & Swank 2002; Blay et al. 2004), and the spin frequency of the neutron star remains fairly constant (Baykal et al. 2007) or slightly decreases (Ducci et al. 2008). In this state the B-type companion shows Hα in absorption (Reig et al.

⋆ E-mail: pau@physics.uoc.gr

Table 1. Hα equivalent width measurements (1σ errors).

Date	Julian date (2,400,000+)	EW(Hα) (Å)	Telescope
SAX J2103.5+4545			
13-09-2012	56184.44	-6.4 ± 0.4	SKO
31-07-2013	56505.39	$+2.4 \pm 0.3$	SKO
30-08-2013	56535.36	$+2.3 \pm 0.2$	SKO
18-10-2013	56584.27	$+1.9 \pm 0.1$	SKO
03-11-2013	56599.62	$+1.9 \pm 0.1$	FLWO
07-12-2013	56634.59	$+1.8 \pm 0.1$	FLWO
06-01-2014	56664.57	$+0.35 \pm 0.05$	FLWO

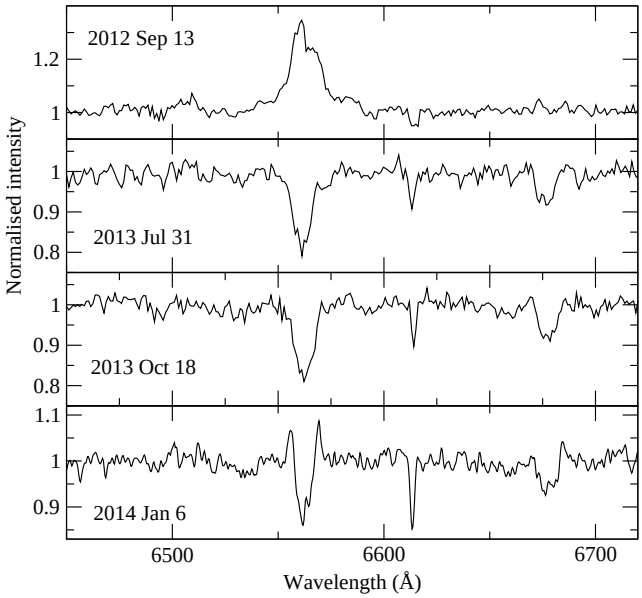

Figure 1. Profile of the Hα line at different epochs. The *Chandra* observations took place on September 9, 2013.

2010; Kızıloğlu et al. 2009), which signifies the recession of the circumstellar Be disk. The average X-ray luminosity in this state is $L_X \sim 3 \times 10^{35}$ erg s^{-1} in the 3–30 keV range (assuming a distance of 6.5 kpc). The bright state generally starts with a sharp flare that lasts for one to two orbital cycles. This flare is then followed by a progressive increase in the X-ray intensity until a maximum is reached at about one order of magnitude brighter than in the faint state. During the bright states, the neutron star spins up (Baykal et al. 2007; Camero Arranz et al. 2007), shows moderate outbursts modulated by the orbital period (Baykal, Stark & Swank 2000; Sidoli et al. 2005), and displays Hα line in emission (Reig et al. 2010; Kızıloğlu et al. 2009), which indicates the growth of the Be disk. The X-ray luminosity at the peak of the outbursts ranges between $(0.6 - 1.0) \times 10^{37}$ erg s^{-1}, while at the peak of the flare the luminosity is typically a factor of 2 higher.

The X-ray spectra of the bright state are distinctly harder than those of the faint state (Baykal, Stark & Swank 2002; Reig et al. 2010). The 1–150 keV X-ray spectra are well represented by an absorbed ($N_{\rm H} \approx \times 10^{22}$ cm^{-2}) power law ($\Gamma_{\rm bright} \approx 0.8 - 1$, $\Gamma_{\rm faint} \approx 1.2 - 1.4$) plus and exponential cutoff at high energy ($E_{\rm cut} \approx 13 - 18$ keV). In addition, a cool iron fluorescence line is observed at 6.4 keV. At lower energy, a soft component consistent with blackbody emission ($kT \approx 1.9$ keV) has been shown to be significant in an *XMM-Newton* observation during a bright state (İnam et al. 2004). This observation also revealed a 44 mHz quasi-periodic oscillation.

In this work we present the results of a timing and spectral analysis of a *Chandra* observation aimed specifically to explore the characteristics of the X-ray emission at very low accretion rates. The source is expected to be in X-ray quiescence when the material in the disk dissipates. Thanks to our regular monitoring of the evolution of the Hα line in the optical spectrum of SAX J2103.5+4545, we were able to trigger the X-ray observations when the line appeared in absorption. The source indeed turned out to be in deep X-ray quiescence with a flux more than two orders of magnitude lower than the faint state previously reported in *RXTE* observations and almost four orders of magnitude lower than during the bright state. We discuss the possible origin of the observed X-ray quiescent emission.

2 OBSERVATIONS

2.1 Optical observations and the Hα line profile

Emission lines in Be stars are the result of recombination radiation from ionised hydrogen in the hot, extended circumstellar envelope surrounding the central Be star. The Hα line is the prime indicator of the circumstellar disk state. In particular, its equivalent width (EW(Hα)) is a robust tracer of the size of the disk (Quirrenbach et al. 1997; Tycner et al. 2005; Grundstrom & Gies 2006). In the absence of the disk, no emission is expected and the line should have the typical photospheric absorption profile.

In this section we present optical spectroscopic observations that demonstrate the absence of the equatorial disk at the time of the X-ray observations. The optical spectroscopic observations were obtained from the Skinakas observatory (SKO) in Crete (Greece) and from the Fred Lawrence Whipple observatory (FLWO) at Mt. Hopkins (Arizona). Table 1 gives the log of the spectroscopic observations and the measured Hα equivalent width. The 1.3 m telescope of the Skinakas Observatory was equipped with a 2000×800 (15 μm) pixel ISA SITe CCD and a 1302 l mm^{-1} grating, giving a nominal dispersion of ∼1 Å/pixel. The FLWO observations were carried out in queue mode with the 1.5-m telescope equipped with the FAST-II spectrograph (Fabricant et al. 1998) and the 1200 l mm^{-1} grating, yielding a dispersion of 0.4Å/pixel. The data were analysed using the RoadRunner package (Tokarz & Roll 1997) implemented in IRAF. Spectra of comparison lamps were taken before each exposure in order to account for small variations of the wavelength calibration during the night.

Our monitoring of SAX J2103.5+4545 reveals that the Hα profile changed from emission into absorption some time around March-May 2013. By convention, the equivalent widths of absorption lines are expressed as positive numbers, while the equivalent widths of emission lines are quoted as negative. Fig. 1 shows the profile of the Hα line at different epochs. In September 2012, a strong emission asymmetric Hα profile with an equivalent width $EW(H\alpha) = -6.4$ Å was measured, indicating the presence of the circumstellar disk. The disk also affected the shape of the HeI line

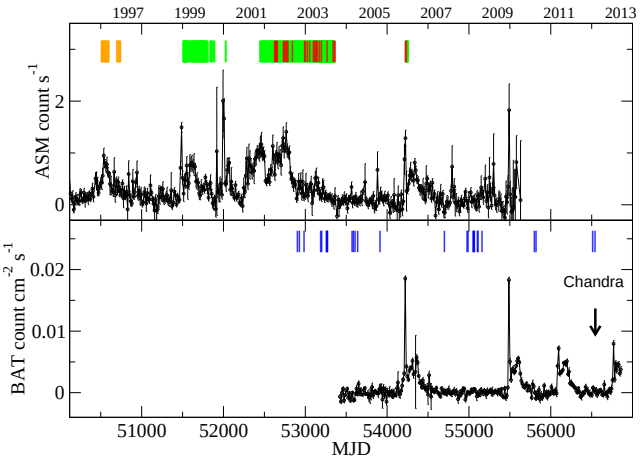

Figure 2. Long-term X-ray variability of SAX J2103.5+4545 as seen by the all-sky monitors *RXTE*/ASM (top) and *SWIFT*/BAT light curves (bottom). The original 1-day resolution light curves were rebinned to a bin size equal to the orbital period ($P_{\rm orb}$ = 12.67 d). The time of published X-ray observations of various missions is indicated in colour as follows: *BeppoSAX* (orange), *RXTE* (green), and *INTEGRAL* (red). The time of the Chandra observation is shown by an arrow. The blue marks in the bottom panel indicate the epochs when the Hα line displayed an absorption profile.

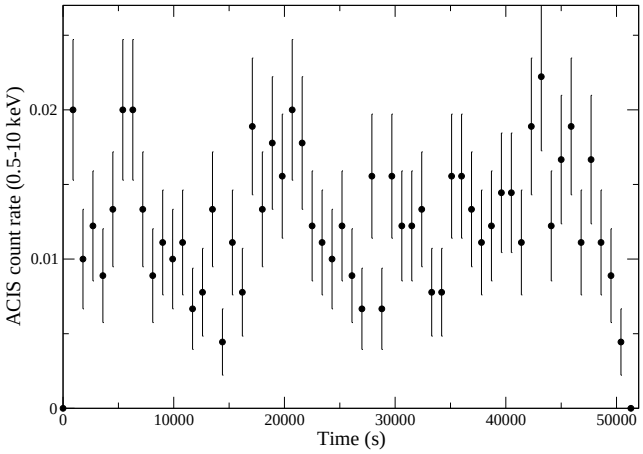

Figure 3. The *Chandra* ACIS light curve binned at a resolution of 900 s in the energy range 0.5–10 keV. Time zero corresponds to MJD 56544.750.

at 6678 Å, which appeared with a double peaked emission profile. About a year later, both lines were observed in absorption, although a very weak peak emerging from the center of the line was observed. This type of profile is known as central quasi-emission peak (CQE) and is an indication of a highly debilitated disk (see Reig et al. 2010, and references therein). On January 6, 2014, the line displayed a double peak shell profile, which implies that the disk is reforming again. The shell feature (central peak below the continuum) suggests that we see the disk at high inclination angle.

2.2 *Chandra* observations

Based on the results of our optical monitoring, we triggered an X-ray observation with *Chandra* on 9 September 2013 (ObsId 15780), when the Hα line was in absorption. A single, uninterrupted 45.4 ks exposure was carried out. The *Chandra* X-ray Observatory is designed for high resolution X-ray imaging and spectroscopy in the energy range 0.2-10 keV (Weisskopf et al. 2002). In this work we used data from the Advanced CCD Imaging Spectrometer (ACIS, Garmire et al. 2003), which provides high resolution (∼1 arcsec) imaging, and moderate spectral (95 eV at 1.5 keV) and timing reslution (∼ 2.85 ms). For our observation, the source was placed at the nominal aim point of the back-illuminated ACIS-S3 CCD. To minimize the possibility of the detector pile up, the observation was performed in a custom subarray mode with 128 pixel rows, starting from CCD row 448 which resulted in the CCD frame time of ∼ 0.04 s. The data reduction and analysis were performed using the CIAO-4.6.1 analysis package and the corresponding calibration products (CALDB version 4.6.1.1).

3 X-RAY ANALYSIS

The source counts were extracted from a circular region of radius ∼ 5 arcsec, centered on the source. The extraction radius was chosen to maximise the signal to noise ratio and encloses ⩾ 98% of the source emission even at high energies. The background was estimated from two source-free circular regions with radius of 22 arcseconds adjacent to the source. The extracted source and background spectra were grouped to contain at least 30 counts per energy bin in the range from 0.2 to 10 keV. For the timing analysis, the photon arrival times were translated to the solar system barycenter and corrected for motion within the binary system using ephemeris reported by Baykal et al. (2007).

3.1 Timing analysis

Figure 2 shows the long-term X-ray light curve of SAX J2103.5+4545, obtained with the *RXTE*/ASM and *Swift*/BAT all-sky monitors. The time of the X-ray observations from various missions is indicated. The ACIS background-subtracted light curve with bin size of 900 s is shown in Fig. 3. The average source count rate after background subtraction is 0.0196 ± 0.0006 counts s^{-1} in the 0.5–10 keV band, while the background count rate is 0.0051 ± 0.0003 counts s^{-1}.

The *Chandra* light curve presented above seems to show some variability on time scales of a few ks with fractional RMS of ∼ 25%. However, variability analysis of the event data using the Gregory-Loredo algorithm (implemented in CIAO tool *glvary*) suggests that the observed emission is consistent with constant rate (the probability of a variable signal is less than 5%).

The power spectrum of the source is also consistent with white noise with the exception of the strong peak detected at the expected period of SAX J2103.5+4545 (see Fig 4). Indeed, the power spectrum of the 1-10 keV light curve with 1 s time bin size reveals a coherent modulation with maximum power at 2.853×10^{-3} Hz, which corresponds to a pulse period of ∼ 351 s (Fig. 4). A more accurate determination of the spin period was obtained through the pulse phase connection technique (Staubert, Klochkov & Wilms 2009). We found the pulse period to be consistent with constant value of 351.13 ± 0.02 s (at 1σ confidence level).

The background subtracted pulse profiles in several energy ranges folded with the obtained period are presented in Fig. 5. The fraction of pulsed emission (defined as $PF = (I_{\rm max} - I_{\rm min})/(I_{\rm max} + I_{\rm min})$, where $I_{\rm min}$ and $I_{\rm max}$, are the minimum and maximum intensity of the pulse profile) is relatively high (50-80%) and independent of energy within the statistical uncertainties. For the 0.5–10 keV band the pulsed fraction is 55 ± 8%. Similar values have been reported for SAX J2103.5+4545 from *XMM-Newton* observations at three

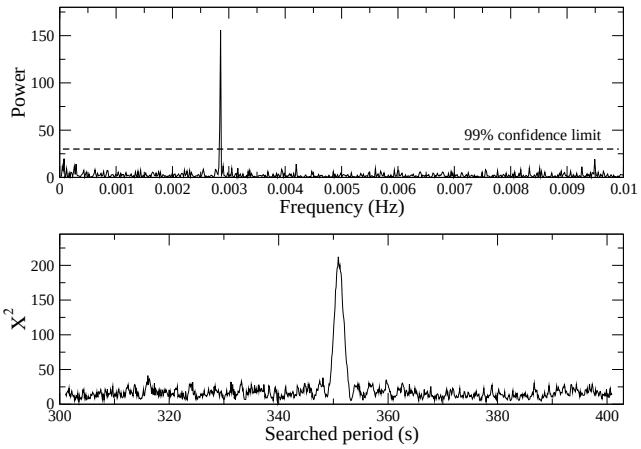

Figure 4. Power spectrum (top) and χ^2 distribution versus folding period. The dashed line marks the 99% confidence detection limit.

orders of magnitude higher luminosity, although the reported pulse shape was different (see Fig. 1 in İnam et al. 2004). The *XMM-Newton* profiles are more asymmetric with a narrow peak followed by a broader one. The overall *Chandra* profiles are more sinusoidal, have only one peak, and cover a larger fraction of the pulse phase with no sharp features.

3.2 X-ray spectral analysis

The source spectrum in the 0.2-10 keV energy range can be fitted ($\chi^2_{\rm red}$ = 1.0 for 7 degrees of freedom) with a single component absorbed blackbody. The blackbody temperature kT = 0.98 ± 0.07 keV, and radius of R = 0.11 ± 0.02 km, assuming a distance of 6.5 kpc, are compatible with the emission from the polar caps of the neutron star. The absorption column of $N_H = (3 \pm 1) \times 10^{21}$ atoms cm^{-2} (assuming abundances by Wilms, Allen & McCray 2000) is roughly compatible with interstellar absorption in the direction of the source ($\sim 6 \times 10^{21}$ Kalberla et al. 2005). The quality of the fit above 6 keV is slightly improved with the inclusion of a power law tail. However, the limited statistics at high energies makes the parameters of the power law unconstrained and the overall improvement in terms of χ^2 not significant.

The 0.5–10 keV unabsorbed X-ray flux is $F_X = 2.3 \times 10^{-13}$ ergs cm^{-2} s^{-1}, which implies an X-ray luminosity of $L_X = 1.2 \times 10^{33}$ ergs s^{-1}, assuming a distance of 6.5 kpc (Reig et al. 2004), or $L_X = 5.6 \times 10^{32}$ ergs s^{-1}, if the distance of 4.5 kpc from X-ray studies is used (Baykal et al. 2007). In either case, this is the lowest luminosity at which X-ray pulsations have been detected in the quiescent state of an accreting pulsar.

4 DISCUSSION

The observational properties and evolution of accreting pulsars are to a large extent defined by the interaction of the magnetosphere of the neutron star with the accreting matter. The magnetosphere size is defined by the magnetic field strength of the neutron star and the ram pressure of the infalling plasma, and becomes large at low accretion rates. For a rotating neutron star this implies that at some point the velocity of the magnetic field lines at the magnetospheric boundary will exceed local Keplerian velocity and the accretion will be inhibited (Illarionov & Sunyaev 1975; Stella, White & Rosner 1986). The X-ray emission is expected to switch off at this point. Further interaction with infalling plasma leads to a spin-down of the neutron star, which is believed to be the key mechanism behind the relatively long observed periods of accreting pulsars (compared with expected birth periods).

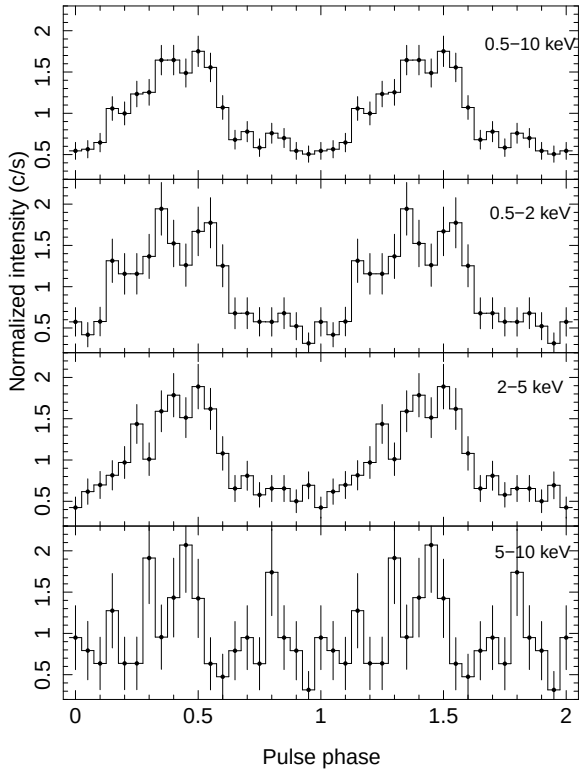

Figure 5. Pulse profile at different energy bands.

Pulsed emission at luminosities $L_X \sim 10^{34}$ erg s^{-1} has been observed in three systems so far (Rutledge et al. 2007). At least in two occasions, 1A 0535+262 (Negueruela et al. 2000; Doroshenko et al. 2014) and IGR J21343+4738 (Reig & Zezas 2014), X-ray pulsed emission was detected during an apparent disk-loss phase. SAX J2103.5+4545 is the third case of pulsations detected during the absence of the Be disk, but it is the first time that X-ray pulsations are detected at a luminosity level of $\sim 10^{33}$ erg s^{-1} in the energy range 0.5–10 keV (see Table 2). In what follows we discuss possible mechanisms that may account for the observed high-energy emission from SAX J2103.5+4545.

The minimal accretion luminosity might be found by imposing $r_m = r_c$, where r_c is the co-rotation radius and r_m the radius of the magnetosphere (see e.g. Campana et al. 2002)

$$L_{\rm min}(R_{\rm NS}) = 3.9 \times 10^{37} k^{7/2} \left(\frac{B}{10^{12}\,{\rm G}}\right)^2 \left(\frac{P_{\rm spin}}{1\,{\rm s}}\right)^{-7/3} \left(\frac{M_{\rm X}}{1.4\ {\rm M}_\odot}\right)^{-2/3} \left(\frac{R_{\rm X}}{10^6\ {\rm cm}}\right)^5\ {\rm erg\,s^{-1}} \quad (1)$$

where k is a constant that accounts for the geometry of the flow. $k \approx 1$ in case of spherical accretion and $k \approx 0.5$ in case of disk accretion (see e.g. Ikhsanov & Beskrovnaya 2010, and references therein). B is the magnetic field strength, $P_{\rm spin}$ the spin period, and $M_{\rm X}$ and $R_{\rm X}$ the mass and radius of the neutron star, respectively.

The long spin period of SAX J2103.5+4545 and the detec-

tion of X-ray pulsations put this source along with 1A 0535+26, 4U 1145–619, and 1A 1118–615, in a category of systems with accretion powered quiescent emission (Rutledge et al. 2007; Doroshenko et al. 2014). Unfortunately, there is no direct estimate of the magnetic field of the neutron star in SAX J2103.5+4545, so it is not clear whether it is in the centrifugally inhibited propeller state. Nevertheless, the fact that pulsed emission is detected suggests that this is likely not the case. We can turn the argument around and derive an upper limit on the magnetic field assuming that the source does not enter the centrifugally inhibited state. For a source distance of 6.5 kpc, $P_{\rm spin} = 351$ s, $k = 1$, and $L_{\rm min} \approx L_{\rm obs} \approx 1.2 \times 10^{33}$ erg s^{-1}, the magnetic field must be $\lesssim 5.2 \times 10^{12}$ G. For higher magnetic fields, $L_{\rm min} > L_{\rm obs}$ and the accreting matter would no longer reach the neutron star surface because it would be spun away by the fast rotation of the magnetosphere.

It is interesting to compare this value with estimates of the magnetic field from the spin evolution history of the pulsar. Based on the correlation of the accreting luminosity and the spin-up rate and the Ghosh & Lamb (1979) model, various authors (Baykal, Stark & Swank 2002; Baykal et al. 2007; Ducci et al. 2008) have estimated the magnetic field to be $B \sim 1 - 3 \times 10^{13}$ G, i.e. the accretion should be inhibited. On the other hand, Sidoli et al. (2005) obtained $B \sim 10^{12}$ G. The uncertainty mainly stems from the distance, which is also a parameter obtained from the fit to the pulse period derivative-luminosity correlation. A magnetic field strength above 10^{13} G requires a distance to the source < 5 kpc. If the distance of 6.5 kpc obtained from optical observations (Reig et al. 2004) is considered, then $B \sim 10^{12}$ G (Sidoli et al. 2005), and the observed X-ray emission might be powered by accretion. In the absence of the Be disk, accretion likely proceeds directly from the stellar wind of the companion. Alternatively, the so-called "dead accretion disks" proposed by Syunyaev & Shakura (1977) might represent another source of matter for accretion.

The main problem with the accretion interpretation is that the X-ray emission is expected to be rather variable regardless of the accretion mechanism, whereas SAX J2103.5+4545 exhibits no detectable variability in the *Chandra* observation. Indeed, all other sources where pulsations have been detected in quiescence (i.e. 4U 1145–619, 1A 1118–615, 1A 0535+26) exhibit strong low frequency noise usually associated with accretion. In fact, SAX J2103.5+4545 exhibits this type of variability as well at higher luminosities (İnam et al. 2004). In contrast, the *Chandra* power spectrum is consistent with white noise with the exception of the pulsation peak.

Of course, with ~ 900 photons detected from the source this might be simply due to the insufficient statistics. To clarify whether this is the case, we have compared our *Chandra* results with the *XMM-Newton* observation of SAX J2103.5+4545 at higher flux level (obsid 0149550401) where the statistics is much better and low frequency noise is apparent. From more than 2×10^5 source photons detected by EPIC PN camera, we randomly selected 900 to match the *Chandra* statistics, and investigated the power spectrum of the resulting light curves. In both cases X-ray pulsations are clearly detected and dominate the power spectrum. To investigate the noise properties we had, therefore, to subtract the pulsed flux from the light curve prior to binning of the power spectrum (Revnivtsev et al. 2009; Doroshenko et al. 2014). In particular, a synthetic lightcurve containing a repeated observation-averaged pulse profile was subtracted from the observed lightcurve, which was sufficient to suppress the observed pulsations below detectability with available statistics. The results are presented in Fig. 7. The excess of power at low frequencies remains apparent in the *XMM-Newton* data set even with the reduced statistics, but it is completely absent in the *Chandra* light curve despite comparable counting statistics (we ignore the background in both cases, which is slightly higher in the *XMM-Newton* observation, so *Chandra* should in fact be even more sensitive to the presence of low frequency noise from the source). We argue, therefore, that the observed change in the power spectrum is likely real and might imply that accretion is not responsible for the observed *Chandra* flux.

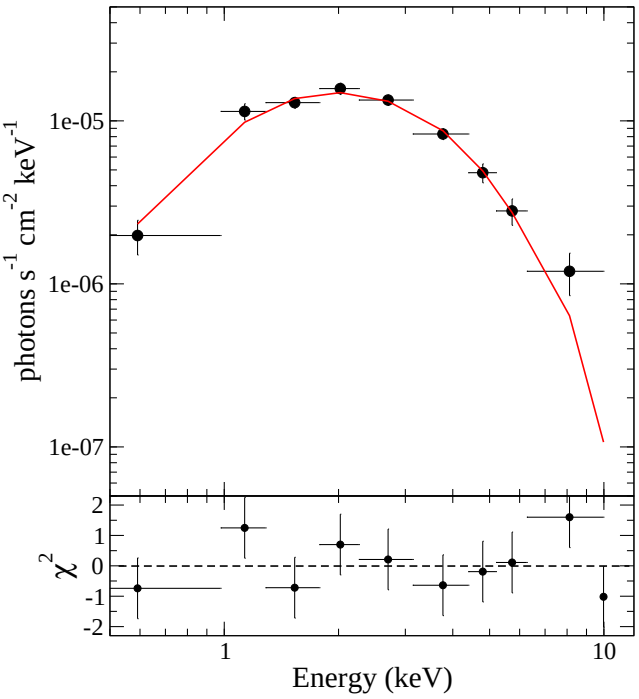

Figure 6. *Chandra*/ACIS-S3 spectrum of SAX J2103.5+4545. The solid line is the best-fitting model composed of an absorbed blackbody.

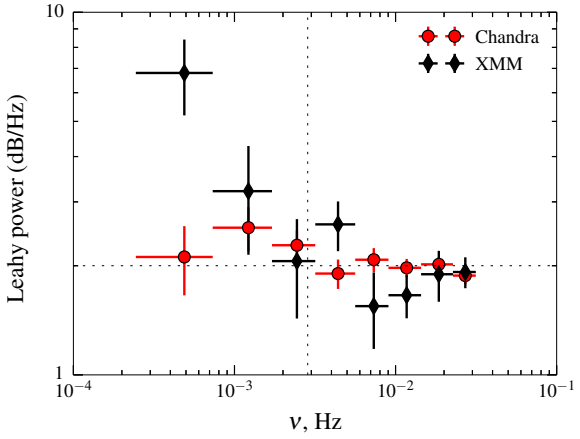

[t]

Figure 7. Comparison of the noise power spectra of SAX J2103.5+4545 at high (*XMM-Newton*) and low (*Chandra*) luminosities. The power is normalized so that the white noise level has a power of two (Leahy et al. 1983), i.e. the *Chandra* lightcurve is consistent with white noise. Counting statistics of the *XMM-Newton* observation was adjusted to match that of *Chandra* as described in the text. Note the absence of the low frequency noise component in *Chandra* power spectrum.

Table 2. Detection of X-rays from Be accreting pulsars at low luminosities.

Source	$P_{\rm spin}$ (s)	L_X (erg s^{-1})	Energy range (keV)	Mission	Distance (kpc)	Equatorial disk	Propoller mechanism
Pulsed emission detected							
SAX J2103.5+4545	351.03 ± 0.05	1.2×10^{33}	0.5–10	*Chandra*[1]	6.5[a]	no	no?
1A 0535+26	103.5	3.5×10^{33}	3–20	*RXTE*[2]	2[b]	no	yes
	103.41 ± 0.02	1.5×10^{33}	2–10	*BeppoSAX*[3,4]	2[b]	yes	yes?
	103.286 ± 0.006	1.3×10^{34}	0.2–12	*XMM-Newton*[5]	2[b]	yes	yes?
4U 1145–619	290 ± 2	5.9×10^{33}	0.5–2	*Einstein*[6]	3.1[c]	yes?	no
1A 1118–615	409.2 ± 0.2	1.8×10^{33}	0.5–10	*Chandra*[7]	5[d]	yes	no
Pulsed emission not detected							
Cep X–4	–	3.2×10^{32}	0.1–2.5	*ROSAT*[8]	3.8[e]	?	yes
4U 0115+63	–	8.4×10^{32}	0.5–10	*BeppoSAX*[9]	8[f]	yes	yes
V 0332+53	–	5.3×10^{32}	0.5–10	*Chandra*[9]	7[g]	yes?	yes
IGR J01363+6610	–	9.1×10^{31}	0.2–12	*XMM-Newton*[10]	2[h]	yes	?
GRO J2058+42	–	5.6×10^{33}	1–10	*Chandra*[11]	9[i]	yes?	?

[1]:this work ; [2]:Negueruela et al. (2000) ; [3]:Orlandini et al. (2004); [4]:Mukherjee & Paul (2005) ; [5]: Doroshenko et al. (2014) ; [6]:Mereghetti et al. (1987) ; [7]:Rutledge et al. (2007) ; [8]: Schulz, Kahabka & Zinnecker (1995) ; [9]:Campana et al. (2002) ; [10]:Tomsick et al. (2011) ; [11]:Wilson et al. (2005) ; [a]:Reig et al. (2004) ; [b]:Steele et al. (1998) ; [c]:Stevens et al. (1997) ; [d]:Janot-Pacheco, Ilovaisky & Chevalier (1981) ; [e]:Bonnet-Bidaud & Mouchet (1998) ; [f]: Reig et al. (2007) ; [g]:Negueruela et al. (1999) : [h]:Reig et al. (2005) ; [i]:Wilson et al. (2005)

Another scenario that has been put forward to explain the quiescent emission of accreting neutron star is deep crustal heating (Brown, Bildsten & Rutledge 1998; Wijnands, Degenaar & Page 2013). During the accretion phase, the crust of a neutron star is heated by nuclear reactions (mainly by beta captures and pycnonuclear reactions). This heat is conducted inwards, heating the core, and outwards, where it is emitted as thermal emission from the surface. After the accreting active period, the crust of a neutron star cools by X-ray emission until it reaches thermal equilibrium with the core emission corresponding to the quiescent state. The X-ray luminosity in this state depends on the time-averaged accretion rate as $L_q \sim 6.03\times10^{32}(\dot{M}/1\times10^{-11}$ M$_\odot$ yr^{-1}), where $\dot{M}$ is the average accretion rate including outbursts (Brown, Bildsten & Rutledge 1998).

To estimate $\dot{M}$ we used the 70-month average *Swift*/BAT spectrum fitting it with a cutoff power law in the 15-100 keV band. The derived source flux is be 3.6×10^{-11} erg cm^{-2} s^{-1}. The average count rate obtained from the 12 year *RXTE*/ASM light curve (see Fig. 2) is 0.3 count s^{-1} or 4 mcrab, which corresponds to a flux of 9.6×10^{-11} erg cm^{-2} s^{-1} in the 2–10 keV band. The overall 1–100 keV luminosity assuming a distance of 6.5 kpc is then 6.5×10^{35} erg s^{-1} and the mass accretion rate $\dot{M} = 5.6\times10^{-11}$ M$_\odot$ yr^{-1}. Here we assumed the canonical mass and radius of a neutron star and maximum efficiency in the conversion of luminosity into mass accretion rate. Thus the time average luminosity in quiescence expected by deep crustal heating is $L_q \sim 3\times10^{33}$ erg s^{-1}, which roughly agrees with the observed value. The problem with the incandescent neutron star scenario is that the blackbody temperature is too high, and the size of the emitting region is too small to be the entire surface of the neutron star (but see discussion in Brown, Bildsten & Rutledge 1998).

The relatively high temperature thermal spectrum, in combination with the large pulse fraction and broad pulse profiles indicate that the emission arises from a rotating region which is hotter (and more luminous) than the rest of the surface of the pulsar. Thus non-uniform cooling, primarily through the polar regions, has to be invoked for this scenario to remain valid. The most obvious explanation is that the observed emission comes from the polar cap, which could be heated by sporadic accretion. Note that our *Chandra* observation took place in between two X-ray outbursts (Fig.2). In this situation, the polar caps does not have the time to cool down.

5 CONCLUSIONS

We have analysed the optical and X-ray emission of the Be/X-ray binary SAX J2103.5+4545 in deep X-ray quiescence. The optical spectra indicate that the Be star's circumstellar disk was absent during the X-ray observation. The X-ray luminosity is the lowest so far observed in this source (more than three orders of magnitude lower than in the bright state) and constitutes the lowest luminosity level for which X-ray pulsations have been detected in an accreting pulsar. The absence of any variability typical for accreting neutron star suggests that the observed emission likely originates from the polar caps of the neutron stars heated during intermittent accretion episodes or by non-uniform cooling of the neutron star after a recent outburst.

ACKNOWLEDGMENTS

VD thank the Deutsches Zentrums für Luft- und Raumfahrt (DLR) and Deutsche Forschungsgemein- schaft (DFG) for financial support (grant DLR 50 OR 0702). This research has made use of software provided by the Chandra X-ray Center (CXC) in the application packages CIAO. This work has made use of NASA's Astrophysics Data System Bibliographic Services and of the SIMBAD database, operated at the CDS, Strasbourg, France. Skinakas Observatory is run by the University of Crete and the Foundation for Research and Technology-Hellas.

REFERENCES

Baykal A., Inam S. Ç., Stark M. J., Heffner C. M., Erkoca A. E., Swank J. H., 2007, MNRAS, 374, 1108

Baykal A., Stark M. J., Swank J., 2000, ApJ, 544, L129

Baykal A., Stark M. J., Swank J. H., 2002, ApJ, 569, 903

Blay P., Reig P., Martínez Núnez S., Camero A., Connell P., Reglero V., 2004, A&A, 427, 293

Bonnet-Bidaud J. M., Mouchet M., 1998, A&A, 332, L9

Brown E. F., Bildsten L., Rutledge R. E., 1998, ApJ, 504, L95

Camero Arranz A., Wilson C. A., Finger M. H., Reglero V., 2007, A&A, 473, 551

Campana S., Stella L., Israel G. L., Moretti A., Parmar A. N., Orlandini M., 2002, ApJ, 580, 389

Corbet R. H. D., 1986, MNRAS, 220, 1047

Doroshenko V., Santangelo A., Doroshenko R., Caballero I., Tsygankov S., Rothschild R., 2014, A&A, 561, A96

Ducci L., Sidoli L., Paizis A., Mereghetti S., Pizzochero P. M., 2008, in Proceedings of the 7th INTEGRAL Workshop

Fabricant D., Cheimets P., Caldwell N., Geary J., 1998, PASP, 110, 79

Garmire G. P., Bautz M. W., Ford P. G., Nousek J. A., Ricker, Jr. G. R., 2003, in Society of Photo-Optical Instrumentation Engineers (SPIE) Conference Series, Vol. 4851, X-Ray and Gamma-Ray Telescopes and Instruments for Astronomy., Truemper J. E., Tananbaum H. D., eds., pp. 28–44

Ghosh P., Lamb F. K., 1979, ApJ, 234, 296

Grundstrom E. D., Gies D. R., 2006, ApJ, 651, L53

Hulleman F., in 't Zand J. J. M., Heise J., 1998, A&A, 337, L25

Ikhsanov N. R., Beskrovnaya N. G., 2010, Astrophysics, 53, 237

Illarionov A. F., Sunyaev R. A., 1975, A&A, 39, 185

İnam S. Ç., Baykal A., Swank J., Stark M. J., 2004, ApJ, 616, 463

Janot-Pacheco E., Ilovaisky S. A., Chevalier C., 1981, A&A, 99, 274

Kalberla P. M. W., Burton W. B., Hartmann D., Arnal E. M., Bajaja E., Morras R., Pöppel W. G. L., 2005, A&A, 440, 775

Kızıloğlu Ü., Özbilgen S., Kızıloğlu N., Baykal A., 2009, A&A, 508, 895

Leahy D. A., Darbro W., Elsner R. F., Weisskopf M. C., Kahn S., Sutherland P. G., Grindlay J. E., 1983, ApJ, 266, 160

Mereghetti S., Bignami G. F., Caraveo P. A., Goldwurm A., 1987, ApJ, 312, 755

Mukherjee U., Paul B., 2005, A&A, 431, 667

Negueruela I., Reig P., Coe M. J., Fabregat J., 1998, A&A, 336, 251

Negueruela I., Reig P., Finger M. H., Roche P., 2000, A&A, 356, 1003

Negueruela I., Roche P., Fabregat J., Coe M. J., 1999, MNRAS, 307, 695

Orlandini M. et al., 2004, Nuclear Physics B Proceedings Supplements, 132, 476

Quirrenbach A. et al., 1997, ApJ, 479, 477

Reig P., 2011, Ap&SS, 332, 1

Reig P., Larionov V., Negueruela I., Arkharov A. A., Kudryavtseva N. A., 2007, A&A, 462, 1081

Reig P., Negueruela I., Fabregat J., Chato R., Blay P., Mavromatakis F., 2004, A&A, 421, 673

Reig P., Negueruela I., Papamastorakis G., Manousakis A., Kougentakis T., 2005, A&A, 440, 637

Reig P., Słowikowska A., Zezas A., Blay P., 2010, MNRAS, 401, 55

Reig P., Zezas A., 2014, MNRAS, submitted

Revnivtsev M., Churazov E., Postnov K., Tsygankov S., 2009, A&A, 507, 1211

Rivinius T., Carciofi A. C., Martayan C., 2013, A&A Rev., 21, 69

Rutledge R. E., Bildsten L., Brown E. F., Chakrabarty D., Pavlov G. G., Zavlin V. E., 2007, ApJ, 658, 514

Schulz N. S., Kahabka P., Zinnecker H., 1995, A&A, 295, 413

Sidoli L. et al., 2005, A&A, 440, 1033

Staubert R., Klochkov D., Wilms J., 2009, A&A, 500, 883

Steele I. A., Negueruela I., Coe M. J., Roche P., 1998, MNRAS, 297, L5

Stella L., White N. E., Rosner R., 1986, ApJ, 308, 669

Stevens J. B., Reig P., Coe M. J., Buckley D. A. H., Fabregat J., Steele I. A., 1997, MNRAS, 288, 988

Syunyaev R. A., Shakura N. I., 1977, Soviet Astronomy Letters, 3, 138

Tokarz S. P., Roll J., 1997, in Astronomical Society of the Pacific Conference Series, Vol. 125, Astronomical Data Analysis Software and Systems VI, Hunt G., Payne H., eds., p. 140

Tomsick J. A., Heinke C., Halpern J., Kaaret P., Chaty S., Rodriguez J., Bodaghee A., 2011, ApJ, 728, 86

Tycner C. et al., 2005, ApJ, 624, 359

Weisskopf M. C., Brinkman B., Canizares C., Garmire G., Murray S., Van Speybroeck L. P., 2002, PASP, 114, 1

Wijnands R., Degenaar N., Page D., 2013, MNRAS, 432, 2366

Wilms J., Allen A., McCray R., 2000, ApJ, 542, 914

Wilson C. A., Weisskopf M. C., Finger M. H., Coe M. J., Greiner J., Reig P., Papamastorakis G., 2005, ApJ, 622, 1024